ISSN 1063-4576, Journal of Superhard Materials, 2023, Vol. 45, No. 1, pp. 20–30. © Allerton Press, Inc., 2023.

PRODUCTION, STRUCTURE, PROPERTIES

Combustion Synthesis of B_4C–TiB_2 Nanocomposite Powder: Effect of Mg Particle Size on SHS and Optimization of Acid Leaching Process

Ozan Coban[a, b, *] (ORCID: 0000-0002-1506-4619), Mehmet Bugdayci[c, d], Serkan Baslayici[a, d], and M. Ercan Acma[a]

[a] *Metallurgical and Materials Engineering Department, Istanbul Technical University, İstanbul, 34467 Turkey*
[b] *Metallurgical and Materials Engineering Department, Istanbul Gedik University, İstanbul, 34876 Turkey*
[c] *Chemical Engineering Department, Yalova University, Yalova, 77200 Turkey*
[d] *Construction Technology Department, Istanbul Medipol University, İstanbul,34810 Turkey*
**e-mail: ozan.coban@gedik.edu.tr*

Received July 18, 2022; revised August 10, 2022; accepted August 15, 2022

Abstract—In this study, composite nanoparticles of B_4C–TiB_2 were produced by combustion synthesis. Production was carried out by self-propagating high-temperature synthesis (SHS) method in atmospheric conditions by using oxide raw materials (B_2O_3, TiO_2), carbon black and magnesium as a reducing agent. The effect of Mg particle size on SHS efficiency was investigated. Single-stage and 2-stage leaching processes were carried out to remove undesired phases in the SHS product. In the 1st HCl acid leaching process, the leaching temperature and leaching duration were optimized. As a result of the 2nd leaching process with the addition of carbonic acid and H_2O_2, commercial quality nanoparticle synthesis was performed. Results revealed that the increase in Mg particle size decreased the SHS efficiency, however very fine particle sized Mg usage decreased the SHS efficiency due to the evaporation and scatter of Mg. The optimum Mg particle size was determined as 75–150 μm. Since it has a significant effect on the removal of Mg-borate phases, 90°C was determined as the optimum leaching temperature. The optimum leaching duration was determined to be 60 min. As a result of optimized leaching processes, 99.11% purity B_4C–TiB_2 nanoparticle with 193.5 nm particle size and 30.65 m^2/g surface area was synthesized.

Keywords: self-propagating high temperature synthesis, boron carbide, titanium diboride, composite powder, nanoparticle synthesis

DOI: 10.3103/S1063457623010033

INTRODUCTION

Synthesis of advanced ceramics is essential for technological developments due to their superior mechanical, thermal, physical and chemical properties. By producing these materials together in a composite structure, the combination of the superior properties of each can be achieved. In terms of providing this, the combustion synthesis method has come to the fore in recent years.

Low density, high hardness, abrasion resistance and strength, and high resistance to chemicals and high temperatures are promising properties of B_4C [1–3]. It is used in armour applications, hard coatings, nuclear applications and as semiconductor in high temperature applications [4–9]. Low toughness, low thermal and electrical conductivity and low sintering ability caused by low plasticity and oxide layer formed on its surface make this material limited in usage [10, 11]. Similarly, TiB_2 has properties such as high melting temperature, high hardness and wear resistance. Although these values are lower than B_4C, it stands out in terms of fracture toughness, thermal shock resistance and chemical stability [12–15]. It has been demonstrated that the fracture toughness, wear resistance and sintering ability can be increased with the combination of these two materials [11, 16].

Many methods for B_4C-TiB_2 production have been studied. Thermal and electric field activated combustion synthesis [17, 18], borothermic reduction [19], carbothermal reduction (using boric acid, carbon black and TiO_2) [20], in situ-synthesis (using boric acid, sugar and $C_8H_{20}O_4Ti$ (titanium(IV) ethanolate)) [21], co-precipitation process [22], sol-gel methods [23] (using B_4C, $TiCl_4$ and Y_2O_3 reactants) have been

reported recently. Combustion synthesis is one of the most significant methods developed for the production of B_4C–TiB_2 composite powder. It eliminates the disadvantages such as requirements for expensive alkoxides, long gelation time, high temperature and/or pressure, extensive mechanical milling, etc. in other methods. Nikzad et al. [24] produced B_4C–TiB_2 by SHS with B, C and Ti elemental raw materials and with Teflon chemical booster for increasing the adiabatic temperature. They also applied mechanical activation process. Usage of elemental raw materials and chemical and mechanical activation increases the production cost. Synthesis from oxide raw materials is significant for cost-efficient production and there are very few studies. Bahabad et al. [25] produced by volume combustion SHS process using B_2O_3, TiO_2, Mg and C. However ignition was provided by continuous argon gas flow at 900°C which increases the cost of process extremely. The latest study conducted by Coban et al. [26] to produce B_4C–TiB_2 nanoparticles economically by using oxide raw materials in atmospheric conditions via SHS method. They investigated the effect of C and Mg mole ratios and charge stoichiometry on SHS process. However, the effect of particle size of reductant, Mg, is another parameter to be investigated.

The particle size of reductant is significant in combustion synthesis according to the kinetic aspect. It is well known that decrease in the particle size increases the surface area which causes higher reaction efficiency. For combustion synthesis, beside thermodynamics, also kinetic principles should be evaluated to understand the effect of particle size. In addition to the thermodynamic criterion put forward by Merzhanov et al. [27] in 1972 and Su et al. [28] in 2014, a new kinetic criterion was put forward by Xiaoming et al. [29] in 2021. They reported that, especially for solid state flame case (where adiabatic temperature is lower than the melting temperature of the reactant which has lower melting point, ($T_{ad}/T_{m,L} < 1$)), the diffusion distance of atoms are needed to be higher than the value of particle size of the reactants, ($l_{Tad} \geq d$). This finding also shows that even the adiabatic temperature is higher, as the particle size decreases, the difference in diffusion distance and particle size increases which causes increase in diffusion rate. Thus, combustion efficiency increases. However, further decrease in particle size could cause evaporation in the case adiabatic temperature is higher than boiling point of reductant ($T_{ad} > T_b$). Although boiling point of reactant is higher than adiabatic temperature, owing to high pressure occurred during combustion synthesis process, the reactants with very fine particle size could be lost due to scattering. Therefore, particle size should be optimized for each system. In combustion synthesis, particle sizes of reactants are highly effective on ignition temperature and time, combustion temperature and rate, velocity of combustion wave, thus combustion synthesis efficiency. Azatyan et al. [30] reported that increase in particle size of Ti caused decrease in combustion temperature and velocity of combustion wave in SHS of Ti–C system. For the system that adiabatic temperature of reaction is lower, particle size is highly effective on occurrence of combustion. Fan et al. [31] found that combustion was complete with usage of Ti with particle size was below 45 μm, while combustion was incomplete with coarser (135–154 μm) Ti usage. Zhang et al. [32] investigated the effect of C particle size in Al–Ti–C system and found that decrease in particle size increased combustion rate and decreased the combustion duration. Similarly, for Ni–Ti–C system, Yang et al. [33] showed that decrease in C particle size was effective on decreasing ignition time and increasing the velocity of combustion wave. For the system of TiO_2–B_2O_3–Mg–C, this study is to be the first for investigating the effect of Mg particle size on SHS process.

Leaching is applied to remove the oxidized phases and other by-products formed after the SHS process. There are some studies on the optimization of the leaching process of TiB_2 and B_4C separately in the literature [34–38]. İpekci et al. [34] investigated the effect of leaching temperature on the chemical content of the TiB_2 product obtained by SHS in TiO_2–B_2O_3–Mg system. They reported that the leaching temperature should be above 70°C in order to remove the Mg-borate phases formed as a by-product. Bilgi et al. [15] reported the same for volume combustion synthesis of TiB_2. Demircan et al. [35] and Turan et al. [38] optimized the acid concentration of the SHS product in HCl leaching and determined 9.3 M concentration as the optimum value for obtaining commercial quality TiB_2 product. For B_4C production, Alkan et al. [37] reported optimum acid concentration as 12.06 M and the solid-to-liquid ratio as 1 : 5 at 80°C. There is no research other than the study by Coban et al. [26] for the optimization of the leaching process in the production of B_4C–TiB_2 by SHS. They determined the optimum acid concentration as 10.5 M for HCl leaching process at 90°C. They also investigated the effect of H_2O_2 and carbonic acid addition on leaching process. However the final product still included undesired phases. The effect of second leaching process should be studied and the other parameters that could affect leaching process, such as temperature and duration, should be optimized.

In this study, B_2O_3, TiO_2, carbon black and Mg powder were used to produce B_4C–TiB_2 composite powder with 50–50% charge stoichiometry by SHS method. Effect of Mg particle size on chemical content of SHS product was investigated. In the HCl leaching process performed following the SHS process,

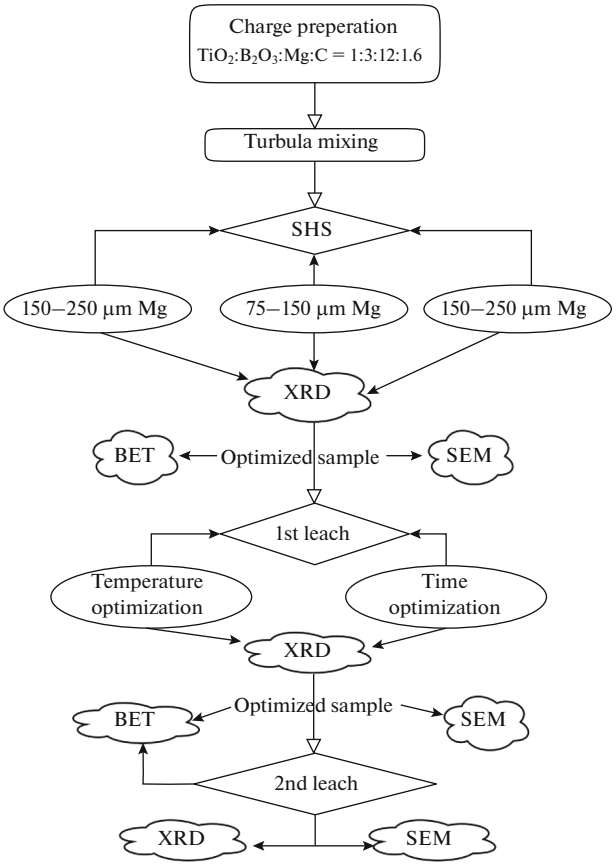

Fig. 1. Flowchart of experimental study.

the leaching temperature and leaching duration were also optimized in this study, as well as the acid concentration optimization performed previously. The effect of the 2-stage leaching process on commercial quality product was also investigated. The novelty of the study is to determine the optimum Mg particle size and optimize the leaching temperature and duration parameters for the production of $B_4C–TiB_2$ by SHS.

EXPERIMENTAL

In this study, $B_4C–TiB_2$ composite powders were produced via SHS process which is a type of combustion synthesis. Following the SHS process, HCl acid leaching was applied. SHS products and leached products were characterized by XRD, SEM and BET analysis. The flowchart of experimental study is given in Fig. 1.

In this study, technical grade TiO_2, Mg and B_2O_3 (obtained by calcination of H_3BO_3, Eti Mine) powders were used in experimental studies. The purity and particle size of raw materials used in the experimental study is given in Table 1. In order to understand the effect of Mg particle size on chemical composition of SHS product, three different Mg raw materials were used in experimental studies with varying particle sizes.

In the study conducted by Coban et al. [26], the effect of mole ratio of Mg and C have been investigated by thermochemical simulation. The estimated phases and adiabatic temperatures have been evaluated. Optimized molar ratios have been determined to be $TiO_2 : B_2O_3 : Mg : C = 1 : 3 : 12 : 1.6$. Also, the charge stoichiometries have been optimized according to the chemical compositions and the best results have been obtained with $B_4C–50$ mol % TiB_2. SHS processes were conducted based on the reaction given in Eq. (1). Thermochemical simulation results revealed that the adiabatic temperature of this reaction is 0°C. $B_4C–TiB_2$ composite powders were produced by SHS method by charging the raw materials into a ladle in a total amount of 100 grams. The optimum stoichiometries of reactants used in experimental studies are given in Table 2.

Table 1. The purity and particle size of raw materials used in the experimental study

Raw materials	Purity, wt %	Particle size, μm
Mg	99.7	150–250/75–150/10–50
B_2O_3	97	<53
TiO_2	98.8	<75
C	98	<30

Table 2. Stoichiometries of reactants used in experimental studies

Sample	Mole ratios and stoichiometric percentage			
	TiO_2	B_2O_3	Mg	C
50% B_4C–50% TiB_2	1	3	12 (110%)	1.6 (160%)

$$TiO_2 + 3B_2O_3 + 11Mg + C \rightarrow TiB_2 + B_4C + 11MgO, \quad (1)$$

After SHS processes, acid leaching was performed in order to dissolve the undesired phases. In the study conducted by Coban et al. [26], optimum HCl concentration has been determined as 10.5 M. In this study, temperature and duration parameters that affect the leaching process were investigated. Thus, the leaching processes were conducted with the conditions given in Table 3. After the first stage leaching process, it was detected that chemical composition was not desirable for industrial usage owing to high amounts of residual Mg, MgO and Mg-borate phases. In order to dissolve these phases, second stage leaching process was applied. However, the second leach process was applied as modified leach which included carbonic acid and H_2O_2 addition. Table 3 presents the second leach experimental conditions. The reason for applying this kind of leaching process has been explained by Coban et al. [26] as carbonic acid and H_2O_2 addition increased the dissolution of TiO_2 and Mg.

In the experimental studies, the prepared raw materials were mixed in a turbula mixer for 10 min, before they were dehumidified at 105°C for 2 h. They were then charged into a copper crucible of which inner diameter was 10 cm and thickness was 2 cm. Owing to its high thermal shock resistance and high toughness, copper crucibles for SHS processes have been used in many studies [39–41]. Cr–Ni wire, which is connected to the DC power supply with a copper cable, is slightly immersed in the upper part of charge. As a result of the exothermic reaction that took place in the area in contact with the wire as a result of applying a voltage of 11–12 V for 3–4 s, the combustion wave rapidly advanced in the direction of the gravitational force. Thus, the process was completed in 10–20 s for 100 g charge. Then, crucible was emerged into water for rapid cooling. Sponge like SHS product was grinded by using agate mortar and leaching processes were applied by using a magnetic stirrer with heater.

For characterization study, XRD, BET and SEM analysis were carried out. PANalytical Aeris X-ray powder Diffractometer (40 kV, 15 mA), Micromeritics ASAP 2020 Surface Area and Porosity Analyzer and Zeiss GeminiSEM 500 Field Emission Scanning Electron Microscope were used for analysis.

Table 3. The conditions of leaching experiments for each sample

Leaching	Acid concentration, M	Leaching temperature, °C	Leaching duration, min	Stirring rate, rpm	Solid : liquid ratio
Single stage leaching	10.5	25/40/65/75/90	30/45/60/75	500 rpm	1 : 5
2nd modified leaching	(10.5 M HCl + Carbonic acid and H_2O_2 addition)	90	60	500 rpm	1 : 5

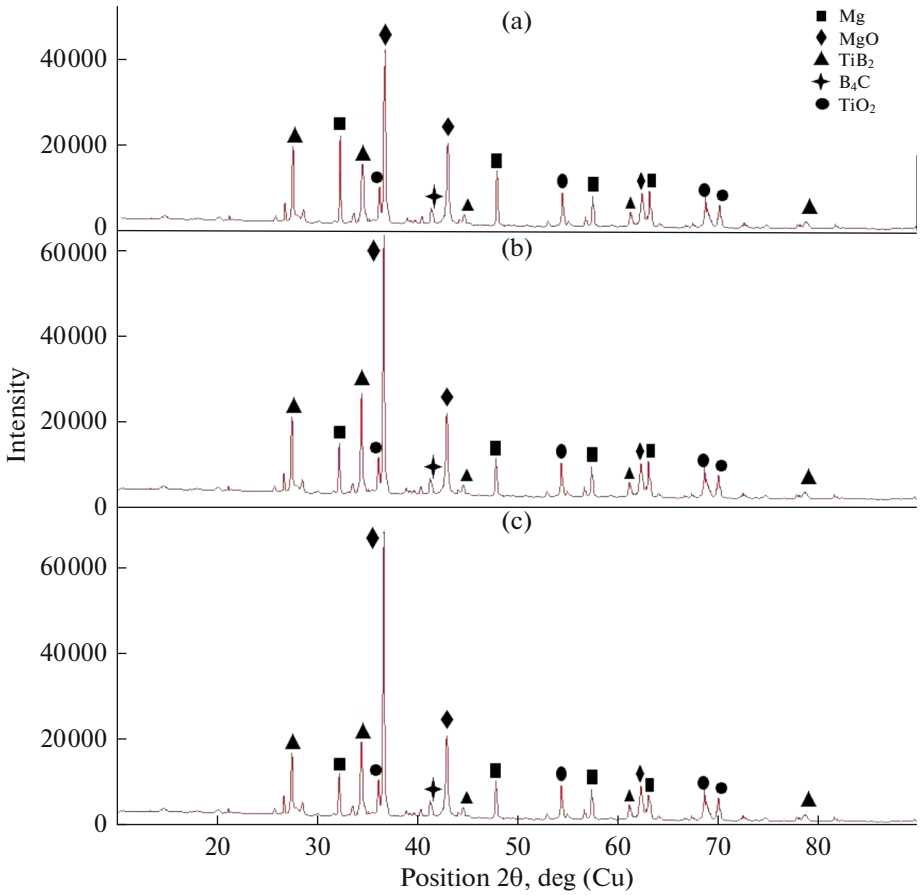

Fig. 2. XRD results of SHS products obtained with varying Mg particle sizes (a) 150–250 μm, (b) 75–150 μm, (c) <50 μm.

RESULTS AND DISCUSSION

Effect of Mg Particle Size on SHS

The XRD results of the products obtained as a result of the SHS process with Mg with 3 different particle sizes are given in Fig. 2. Figure 3 shows the contents of B_4C–TiB_2, Mg and MgO in the product as a result of SHS with varying Mg particle size. As can be seen in Figs. 2a and 3, as Mg particle size increased up to 150–250 μm, the amount of MgO and B_4C–TiB_2 decreased, while the amount of Mg increased in the SHS product. As the Mg particle size increased, the SHS efficiency decreased due to the increment in ignition temperature. The amount of residual Mg which has not participated in reaction increased. Yu'nan et al. [42] reported that decrease in the particle size provided higher combustion intensity, self-sustaining combustion time and burn-off rate. As can be seen in Figs. 2c and 3, as the Mg particle size decreased, the amount of B_4C–TiB_2 decreased, although the amount of MgO increased. That is, Mg has been oxidized but the reduction efficiency has decreased. Very fine grained magnesium formed a very high combustion temperature and pressure, some Mg evaporated, scattered and burned with the oxygen present in the reaction medium to form MgO. In other words, it did not increase the magnesiothermic reduction efficiency. It can be said that further reducing the particle size will have a positive effect in the case of working in an argon atmosphere, but it has a negative effect in the case of performing SHS under atmospheric conditions. According to the results, the optimized Mg particle size was determined to be 75–150 μm for B_4C–TiB_2 particle synthesis via SHS with oxide raw materials and Mg and C usage.

Effect of Acid Leaching Temperature

With the determined optimum acid concentration, HCl leaching was carried out at different temperatures and the phase contents in the obtained products were determined. The results obtained as a result of the analysis performed on the SHS product before leaching are given in Table 1. As can be seen from

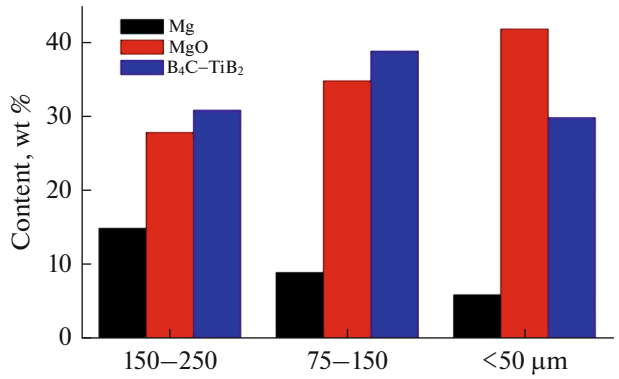

Fig. 3. Effect of Mg particle size on phase content of SHS product.

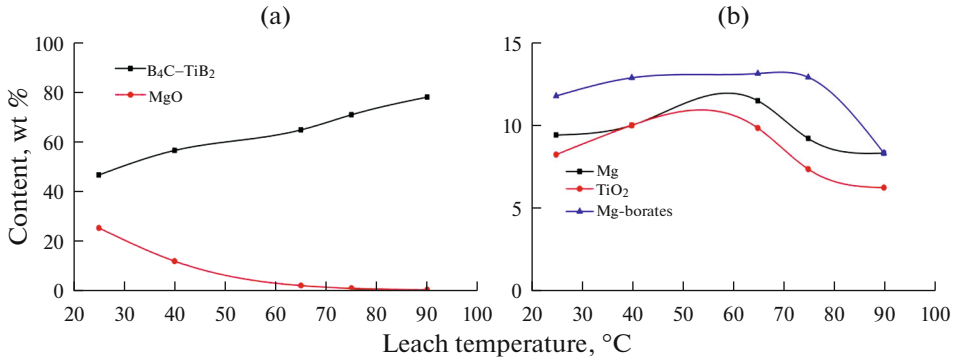

Fig. 4. Effect of leaching temperature on content of 1st leach product.

Fig. 4a, MgO removal efficiency increased significantly as the leaching temperature increased. While the amount of MgO decreased from 35 to 24% by leaching at room temperature, its complete removal (0.017%) was only achieved at 75°C. As can be seen in Fig. 4b, the removal of Mg, TiO_2 and Mg-borate phases were very low up to 65°C. The increase in their ratio here is due to the removal of MgO. The dissolution efficiency of Mg and TiO_2 increased only by lowering the MgO activity in the solution at 65°C. In accordance with the results of Ipekci et al. [34], Mg-borate phases, on the other hand, could be dissolved above 75°C, but a significant amount of Mg-borate phases remained in the product even at 90°C. Ipekci et al. studied on SHS of TiB_2 while this study was on SHS of B_4C–TiB_2 which makes the charge amount of borate forming oxides (B_2O_3) to be higher. The reason for the increase in the dissolution rate of Mg and TiO_2 above 75°C is that the Mg-borates started to decrease significantly. For all these reasons, the optimum leaching temperature was determined as 90°C.

Effect of Acid Leaching Duration

Phase analysis was performed on the leach products by performing leaching processes at varying durations at optimized acid concentration and leaching temperature conditions. According to the results given in Figs. 5a, 5b, dissolution was achieved at very low rates over 60 min. The optimum leaching duration was determined as 60 min.

Table 4. Phase analysis result of SHS product before leaching process

Phases	Mg	MgO	TiO_2	Mg-borate	B_4C–TiB_2
Content, wt %	9	35	7	10	39

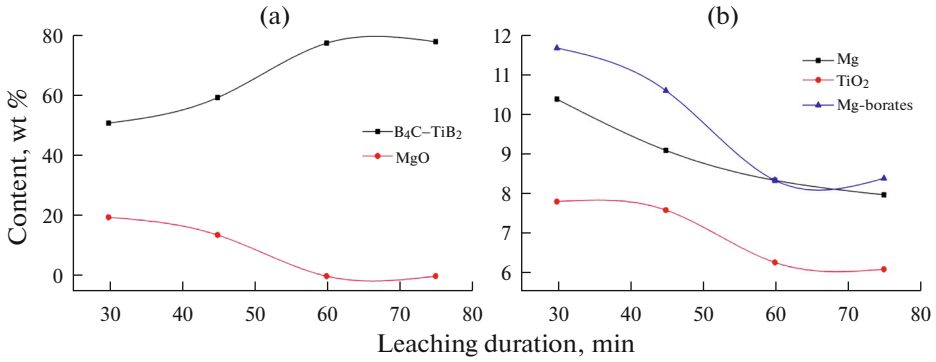

Fig. 5. Effect of leaching duration on phase content of 1st leach product.

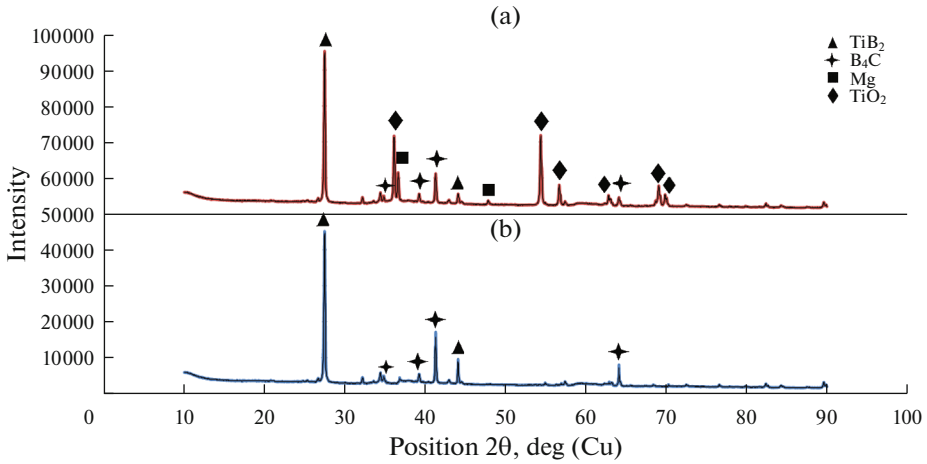

Fig. 6. XRD results of (a) 1st leach product, (b) modified 2-stage leach product.

Effect of Modified Second Leach

After determining the optimum acid concentration, temperature and time, modified second leaching process was applied to the obtained leaching product. The effect of the second leach process is shown with XRD analysis in Fig. 6. Accordingly, TiO_2 and residual Mg, which could not be removed in the single-stage leaching process, could be dissolved. Mg-borate phases were also largely removed. The phase analysis results of the obtained product are shown in Fig. 7. According to the results, 99.11% purity B_4C–TiB_2 composite powder could be obtained as a result of 2-stage leaching process.

SEM micrographs of SHS product, single-stage leached product and modified 2nd leaching applied product of 50% B_4C–50% TiB_2 sample are given in Figs. 8a–8c, respectively. It was observed that leaching process significantly reduced the particle size and increased the surface area. BET analysis results given in Table 5 also revealed it. Figure 8c revealed that 2-stage leaching process provided the dissolution of undesired phases. In addition, leaching process significantly increased porosity. It was also observed that modified 2nd leaching process slightly increased the surface area and pore volume and slightly decreased the particle size.

Table 5. BET analysis results

Product	BET surface area, m^2/g	Average particle size, nm	Pore volume, cm^3/g
SHS product	1.6133	3719	0.0128
1st leach	28.8037	208.3	0.1551
Modified 2nd leach	30.6523	193.5	0.1773

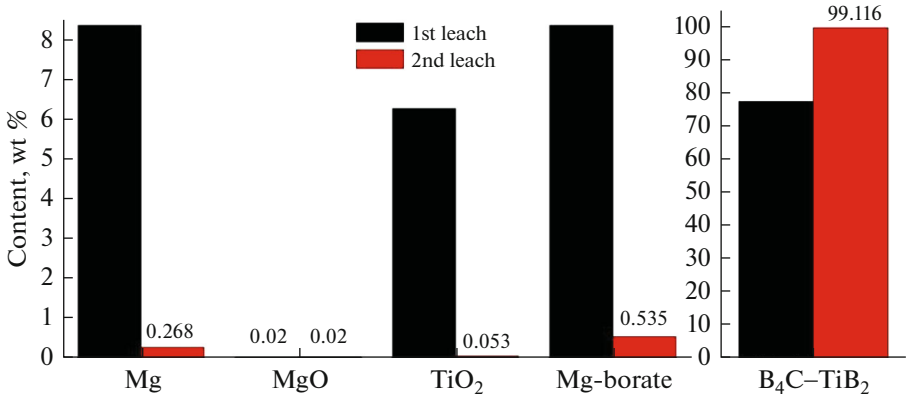

Fig. 7. Effect of second leach application on phase content.

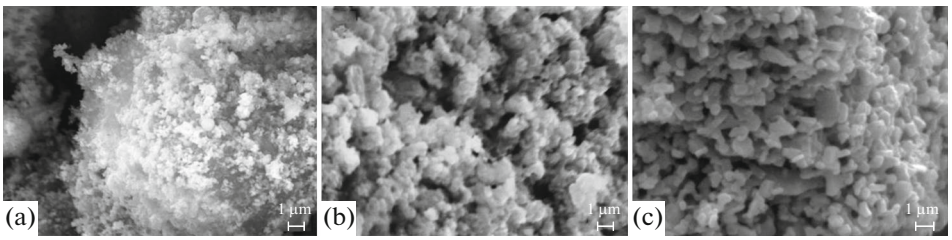

Fig. 8. SEM micrographs of (a) SHS product, (b) 1st leach product, (c) modified 2nd leach product (magnification, ×10000).

CONCLUSIONS

In this study, the synthesis of nanocomposite powders of $B_4C–TiB_2$, which has an important place among advanced technology ceramic materials, by SHS, which is one of the combustion synthesis methods, was studied. The effect of particle size of Mg used as a reducing agent on the SHS process was investigated. In addition, the effects of temperature and time on the phase amounts of the product, which are parameters affecting the leaching process after SHS, were investigated. According to the results obtained:

• By increasing the Mg particle size above 150 μm, the amount of unreacted Mg in the product increased owing to the decrease in reaction surface area in combustion synthesis. Therefore, the SHS efficiency decreased and the amount of $B_4C–TiB_2$ in SHS product decreased.

• Although the amount of unreacted Mg decreased with the decrease in Mg particle size below 50 μm, the amount of $B_4C–TiB_2$ also decreased. The increase in the amount of MgO showed that the high pressure formation in the combustion synthesis caused the scatter of Mg. As a result of combustion with oxygen in the environment, the amount of MgO increased. For these reasons, 75–150 μm was determined as the optimum Mg particle size.

• The increase in leaching temperature continuously decreased the amount of MgO and increased the amount of $B_4C–TiB_2$. It has been determined that Mg-borate phases could not be dissolved especially below 75°C, and Mg and TiO_2 could be dissolved above 65°C. Since the dissolution rate of the Mg-borate phase continued to increase, the optimum leaching temperature was determined as 90°C. It can be applied at 75–80°C depending on the operating conditions of facility.

• The optimum leaching duration for synthesis of $B_4C–TiB_2$ nanocomposite powder by SHS was determined as 60 min. The leaching application at higher duration values did not affect the amount of desired $B_4C–TiB_2$ phase and undesired Mg, MgO, Mg-borates and TiO_2 phases in the product.

• It was determined that second leaching application is essential for the synthesis of $B_4C–TiB_2$ nanocomposite powder by SHS in atmospheric conditions due to the fact that second leaching with added carbonic acid and H_2O_2 had a significant effect on the removal of Mg and TiO_2. It had little effect on particle size, surface area and pore volume.

The results revealed that commercial quality, 99.11% purity $B_4C–TiB_2$ nanoparticle powder with 193.5 nm particle size and 30.65 m^2/g surface area could be synthesized by the route of SHS and then 2-stage HCl leaching using oxide raw materials and Mg and C under atmospheric conditions.

ACKNOWLEDGMENTS

The authors are grateful to Dr. Amir Motallebzadeh from Koç University Surface Science and Technology Center (KUYTAM) for BET Surface Area Analysis.

FUNDING

The study was supported by the Yalova University within the scope of the Scientific Research Project "Production of Nano Composites of Boron Carbide–Titanium Diboride ($B_4C–TiB_2$) by Self-Propagating High Temperature Synthesis (SHS)," project no. 2022/AP/0002.

CONFLICT OF INTEREST

The authors declare that they have no conflicts of interest.

AUTHOR CONTRIBUTIONS

All authors contributed to the study conception and design. Material preparation, data collection and analysis were performed by Ozan Coban, Serkan Baslayici, Mehmet Bugdayci and M. Ercan Acma. The first draft of the manuscript was written by Ozan Coban and all authors commented on previous versions of the manuscript. All authors read and approved the final manuscript.

REFERENCES

1. Dariel, M.P. and Frage, N., Reaction bonded boron carbide: Recent developments, *Adv. Appl. Ceram.*, 2012, vol. 111, nos. 5–6, pp. 301–310. https://doi.org/10.1179/1743676111Y.0000000078
2. Xin, L., Minjun, L., Shuaibo, G., Shu, Y., Xiaofeng, W., and Pengfei, X., Effect of initial compositions on boron carbide synthesis and corresponding growth mechanism, *Adv. Appl. Ceram.*, 2019, vol. 118, no. 8, pp. 442–450. https://doi.org/10.1080/17436753.2019.1664792
3. Yaşar, Z.A. and Haber, R.A., Effect of sintering temperature and applied pressure on the properties of boron carbide-silicon carbide composites, *J. Superhard Mater.*, 2021, vol. 43, pp. 392–404. https://doi.org/10.3103/S1063457621060022
4. Crouch, I.G. and Eu, B., *The Science of Armour Materials*, vol. 11: *Ballistic Testing Methodologies*, New York: Woodhead, 2017, pp. 639–673. https://doi.org/10.1016/B978-0-08-100704-4.00011-6
5. Domnich, V., Reynaud, S., Haber, R., and Chhowalla, M., Boron carbide: Structure, properties and stability under stress, *J. Am. Ceram. Soc.*, 2011, vol. 64, no. 11, pp. 3605–3628. https://doi.org/10.1111/j.1551-2916.2011.04865.x
6. Savio, S.G., Sambasiva Rao, A., Rama Subba Reddy, P., and Madhu, V., Microstructure and ballistic performance of hot pressed & reaction bonded boron carbides against an armour piercing projectile, *Adv. Appl. Ceram.*, 2019, vol. 118, no. 5, pp. 264–273. https://doi.org/10.1080/17436753.2018.1564416
7. Wood, C., Materials for thermoelectric energy conversion, *Rep. Prog. Phys.*, 1988, vol. 51, no. 4, p. 459. https://doi.org/10.1088/0034-4885/51/4/001
8. Suri, A.K., Subramanian, C., Sonber, J.K., and Murthy, T.S.R.Ch., Synthesis and consolidation of boron carbide: a review, *Int. Mater. Rev.*, 2010, vol. 55, no. 1, pp. 4–40. https://doi.org/10.1179/095066009X12506721665211
9. Sauerschnig, P., Watts, J.L., Vaney, J.B., Talbot, P.C., Alarco, J.A., Mackinnon, I.D.R., et al., Thermoelectric properties of phase pure boron carbide prepared by a solution-based method, *Adv. Appl. Ceram.*, 2020, vol. 119, no. 2, pp. 97–106. https://doi.org/10.1080/17436753.2019.1705017
10. Madhav Reddy, K., Guo, J.J., Shinoda, Y., Fujita, T., Hirata, A., Singh, J.P., et al., Enhanced mechanical properties of nanocrystalline boron carbide by nanoporosity and interface phases, *Nat. Commun.*, 2012, vol. 3, no. 1052. https://doi.org/10.1038/ncomms2047

11. Heydari, M.S. and Baharvandi, H.R., Comparing the effects of different sintering methods for ceramics on the physical and mechanical properties of B_4C–TiB_2 nanocomposites, *Int. J. Refract. Met. Hard Mater.*, 2015, vol. 51, pp. 224–232. https://doi.org/10.1016/j.ijrmhm.2015.04.003
12. Mukhopadhyay, A., Raju, G.B., Basu, B., and Suri, A.K., Correlation between phase evolution, mechanical properties and instrumented indentation response of TiB_2-based ceramics, *J. Eur. Ceram. Soc.*, 2009, vol. 29, no. 3, pp. 505–516. https://doi.org/10.1016/j.jeurceramsoc.2008.06.030
13. Ricceri, R. and Matteazzi, P., A fast and low-cost room temperature process for TiB_2 formation by mechanosynthesis, *Mater. Sci. Eng., A*, 2004, vol. 379, nos. 1–2, pp. 341–346. https://doi.org/10.1016/j.msea.2004.02.064
14. Górnya, G., Rączkaa, M., Stobierskia, L., Rożniatowskib, K., and Rutkowskia, P., Ceramic composite Ti_3SiC_2–TiB_2-Microstructure and mechanical properties, *Mater. Charact.*, 2009, vol. 60, no. 10, pp. 1168–1174. https://doi.org/10.1016/j.matchar.2009.03.011
15. Bilgi, E., Camurlu, H.E., Akgun, B., Topkaya, Y., and Sevinc, N., Formation of TiB_2 by volume combustion and mechanochemical process, *Mater. Res. Bull.*, 2008, vol. 43, no. 4, pp. 873–881. https://doi.org/10.1016/j.materresbull.2007.05.001
16. Ivzhenko, V.V., Kryl', A.O., Kryl', Y.A. et al., Study of aeroabrasive wear of hot-pressed materials of the B_4C–TiB_2 system, *J. Superhard Mater.,* 2014, vol. 36, pp. 187–192. https://doi.org/10.3103/S106345761403006X
17. Munir, Z.A. and Anselmi-Tamburini, U., Self-propagating exothermic reactions: The synthesis of high-temperature materials by combustion, *Mater. Sci. Rep.*, 1989, vol. 3, nos. 7–8, pp. 277–365. https://doi.org/10.1016/0920-2307(89)90001-7
18. Xue, H. and Munir, Z.A., Extending the compositional limit of combustion synthesized B_4C–TiB_2 composites by field activation, *Metall. Mater. Trans. B*, 1996, vol. 27, pp. 475–480.
19. Fard, H.S.P., Baharvandi, H.R., Abdizadeh, H., and Shahbahrami, B., Chemical synthesis of nano-titanium diboride powders by borothermic reduction, *Int. J. Mod. Phys. B*, 2008, vol. 22, nos. 18–19, pp. 3179–3184. https://doi.org/10.1142/S0217979208048085
20. Pei, L.Z. and Xiao, H.N., B_4C–TiB_2 composite powders prepared by carbothermal reduction method, *J. Mater. Process. Technol.*, 2009, vol. 209, no. 4, pp. 2122–2127. https://doi.org/10.1016/j.jmatprotec.2008.05.003
21. Cakir, E., Ergun, C., Sahin, F.C., and Erden, I., In situ synthesis of B_4C/TiB_2 composites from low cost sugar based precursor, *Defect Diffus. Forum*, 2010, vols. 297–301, pp. 52–56. https://doi.org/10.4028/www.scientific.net/DDF.297-301.52
22. Hongqiang, R., Haifei, X., Liang, Y., Peng, L., Xiaodong, L., and Guanming, Q., Microstructure of TiB_2/B_4C composites with 1% Y_2O_3 prepared by co-precipitating and in situ synthesis, *J. Rare Earths*, 2007, vol. 25, no. 1, pp. 42–45. https://doi.org/10.1016/S1002-0721(07)60520-1
23. Biedunkiewicz, A., Figiel, P., Gabriel, U., Sabara, M., and Lenart, S., Synthesis and characteristics of nanocrystalline materials in Ti, B, C and N containing system, *Cent. Eur. J. Phys.*, 2011, vol. 9, no. 2, pp. 417–422. https://doi.org/10.2478/s11534-010-0121-x
24. Nikzad, L., Licheri, R., Vaezi, M.R., Orrù, R., and Cao, G., Chemically and mechanically activated combustion synthesis of B_4C–TiB_2 composites, *Int. J. Refract. Met. Hard Mater.*, 2012, vol. 35, pp. 41–48. https://doi.org/10.1016/j.ijrmhm.2012.04.001
25. Shojaie Bahaabad, M., Mechanically activated combustion synthesis of B_4C–TiB_2 nanocomposite powder, *J. Adv. Mater. Process.*, 2017, vol. 5, no. 1, pp. 13–21.
26. Coban, O., Bugdayci, M., and Acma, M.E., Production of B_4C–TiB_2 composite powder by self-propagating high-temperature synthesis, *J. Aust. Ceram. Soc.*, 2022, vol. 58, pp. 777–791. https://doi.org/10.1007/s41779-022-00714-5
27. Merzhanov, A.G. and Borovinskaya, I.P., Self-spreading high-temperature synthesis of refractory compounds, *Dokl. Chem.*, 1972, vol. 204, no. 2, pp. 429–431.
28. Su, X.L., Fu, F., Yan, Y.G., Zheng, G., Liang, T., Zhang, Q., et al., Self-propagating high-temperature synthesis for compound thermoelectrics and new criterion for combustion processing, *Nat. Commun.*, 2014, vol. 5, p. 4908. https://doi.org/10.1038/ncomms5908
29. Xiaoming, T., Xianli, S., Yonggao, Y., Ctirad, U., Qingjie, Z., and Xinfeng, T., New criteria for the applicability of combustion synthesis: The investigation of thermodynamic and kinetic processes for binary chemical reactions, *J. Alloys Compd.*, 2021, vol. 860, p. 158465. https://doi.org/10.1016/j.jallcom.2020.158465

30. Azatyan, T.S., Mal'stev, V.M., Merzhanov, A.G., and Seleznev, V.A., Spectral-optical investigation of the mechanism of the combustion of mixtures of titanium and carbon, *Combust., Explos., Shock Waves*, 1977, vol. 13, pp. 156–158.
31. Fan, Q.C., Chai, H.F., and Jin, Z.H., Effects of particle size of reactant on characteristics of combustion synthesis of TiC-Fe cermet, *J. Mater. Sci.*, 2002, vol. 37, pp. 2251–2257.
32. Zhang, E.L., Zeng, S.Y., Yang, B., Li, Q.C., and Ma, M.Z., A study on the kinetic process of reaction synthesis of TiC: Part I. Experimental research and theoretical model, *Metall. Mater. Trans. A*, 1999, vol. 30, pp. 1147–1151.
33. Yang, Y.F., Wang, H.Y., Zhao, R.Y., Liang, Y.H., Zhan, L., and Jiang, Q.C., Effects of C particle size on the ignition and combustion characteristics of the SHS reaction in the 20 wt % Ni–Ti–C system, *J. Alloys Compd.*, 2008, vol. 460, pp. 276–282.
34. İpekci, M., Acar, S., Elmadağlı, M., Hennicke, J., Balcı, Ö., and Somer, M., Production of TiB_2 by SHS and HCl leaching at different temperatures: Characterization and investigation of sintering behavior by SPS, *Ceram. Int.*, 2017, vol. 43, no. 2, pp. 2039–2045. https://doi.org/10.1016/j.ceramint.2016.10.174
35. Demircan, U., Derin, B., and Yücel, O., Effect of HCl concentration on TiB_2 separation from a self-propagating high-temperature synthesis (SHS) product, *Mater. Res. Bull.*, 2007, vol. 42, pp. 312–318.
36. Lok, J.Y., Logan, K.V., and Payyapilly, J.J., Acid leaching of SHS produced magnesium oxide/titanium diboride, *J. Am. Ceram. Soc.*, 2009, vol. 92, pp. 26–31. https://doi.org/10.1111/j.1551-2916.2008.02835.x
37. Alkan, M., Sonmez, M.S., Derin, B., and Yucel, O., Effect of initial composition on boron carbide production by SHS process followed by acid leaching, *Solid State Sci.*, 2012, vol. 14, nos. 11–12, pp. 1688–1691. https://doi.org/10.1016/j.solidstatesciences.2012.07.004
38. Turan, A., Bugdayci, M., and Yucel, O., Self-propagating high temperature synthesis of TiB_2, *High Temp. Mater. Processes*, 2015, vol. 34, no. 2, pp. 185–193. https://doi.org/10.1515/htmp-2014-0021
39. Alkan, M., Sonmez, M.S., Derin, B., Yucel, O., Andreev, D., Sanin, V., et al., Production of Al-Co-Ni ternary alloys by the SHS method for use in nickel based superalloys manufacturing, *High Temp. Mater. Processes*, 2015, vol. 34, no. 3, pp. 275–283. https://doi.org/10.1515/htmp-2014-0052
40. Yucel, O., Bugdayci, M., and Turan, A., Recent ferroalloy studies at Istanbul Technical University, *KnE Mater. Sci.*, 2019, vol. 5, no. 1, pp. 101–107. https://doi.org/10.18502/kms.v5i1.3956
41. Moghaddam, S., Derin, B., Yucel, O., Sonmez, M., Sezen, M., Bakan, F., et al., Production of Mo_2NiB_2 based hard alloys by self-propagating high-temperature synthesis, *High Temp. Mater. Processes*, 2019, vol. 38, pp. 683–691. https://doi.org/10.1515/htmp-2019-0020
42. Yu'nan, Z., Jianzhong, L., Daolun, L., Wei, S., Weijuan, Y., and Junhu, Z., Effect of particle size and oxygen content on ignition and combustion of aluminum particles, *Chin. J. Aeronaut.*, 2017, vol. 30, no. 6, pp. 1835–1843. https://doi.org/10.1016/j.cja.2017.09.006